ELSEVIER

Geomorphology 42 (2002) 255–278

GEOMORPHOLOGY

www.elsevier.com/locate/geomorph

Neotectonics and Quaternary geology of the Hunter Mountain fault zone and Saline Valley region, southeastern California

John A. Oswald *, Steven G. Wesnousky

Center for Neotectonic Studies, Department of Geological Sciences, University of Nevada, Reno, Nevada 89557, USA

Received 14 May 1999; received in revised form 11 May 2001; accepted 14 May 2001

Abstract

The Hunter Mountain fault zone strikes northwesterly, is right-lateral strike-slip, and kinematically links the northern Panamint Valley fault zone to the southern Saline Valley fault zone. The most recent displacement of the fault is recorded in the offset of Holocene deposits along the entire length of the fault zone. Right-lateral offsets of drainage channels within Grapevine Canyon reach up to 50 to 60 m. Initial incision of the offset channels is interpreted on the basis of geomorphic and climatic considerations to have occurred approximately 15 ka. The 50 to 60 m of offset during 15 ka corresponds to a right-lateral fault slip rate of 3.3–4.0 mm/year within Grapevine Canyon. Further to the north along the Nelson Range front, the fault is composed of two sub-parallel fault strands and the fault begins to show an increased normal component of motion. A channel margin that is incised into a Holocene surface that is between 10 and 128 ka in age is offset 16–20 m, which yields a broad minimum bound on the lateral slip rate of 0.125–2.0 mm/year. The best preserved single-event displacements recorded in Holocene deposits range from 1.5 to 2.5 m. In addition to faulting within Grapevine Canyon and the main rangefront fault along the southwest edge of Saline Valley, there also exist normal fault strands within the Valley that strike northeasterly and towards Eureka Valley. The northeasterly striking normal faults in the Valley appear to be actively transferring dextral slip from the Hunter Mountain fault zone north and east onto the Furnace Creek fault zone. Separations on northerly trending, normal faults within Saline Valley yield estimates of slip rates in the hundredths of millimeters per year.

Keywords: Quaternary; Geomorphology; Neotectonics; Earthquakes

1. Introduction

The Hunter Mountain fault zone and Saline Valley are located in southeastern California (Fig. 1). Within the Basin and Ranges Province, the study area is situated at the boundary between the Mojave and Great Basin deserts and, tectonically, within the southern Walker Lane. The Hunter Mountain fault zone is primarily strike-slip in nature and accommodates a portion of relative motion between the Pacific and North American Plates (Dokka and Travis, 1990; Ward, 1990). The only quantitative geologic constraint on the slip rate of the fault arises from the work of Burchfiel et al. (1987). He estimated the long-term slip rate of the fault to equal 2–3 mm/year based

* Corresponding author. GeoEngineers Inc., 2259 Myrtle Avenue, Eureka, CA 95570, USA.

E-mail addresses: joswald@geoengineers.com (J.A. Oswald), stevew@seismo.unr.edu (S.G. Wesnousky).

0169-555X/02/$ - see front matter
PII: S0169-555X(01)00089-7

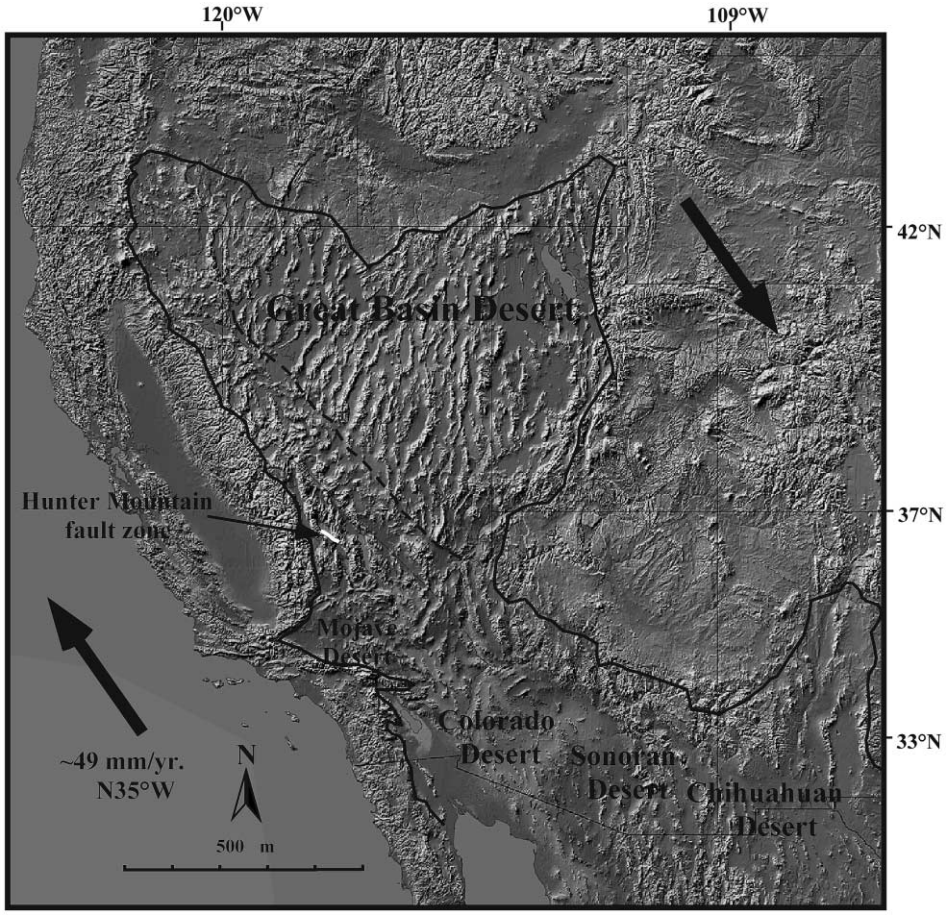

Fig. 1. The Hunter Mountain fault zone and Saline Valley are situated within the Basin and Range province (black outline) of the western United States near the boundary between the Great Basin and Mojave Deserts. The valley and fault are tectonic elements of the southern Walker Lane Belt. The Hunter Mountain fault zone takes up a portion of the dextral relative motion (large arrows) between the Pacific and North American plates (plates rate from DeMets et al., 1990).

on the offset of a piercing point defined by the contact of 3–4 Ma basalts and underlying Hunter Mountain Batholith. The absence of an estimate of a Quaternary slip rate for the fault motivated us to map in detail the neotectonic character of the Hunter Mountain fault zone and the adjacent and offset Quaternary deposits. In this paper, we present surficial geologic maps of five sections along the fault zone. The map observations are then used to place loose bounds on the paleoearthquake history and fault slip rate in late Quaternary time, as well as the role the fault zone plays in the accommodation of slip through the southern Walker Lane (Fig. 2).

2. Geotectonic framework

The Hunter Mountain fault zone kinematically links the northern Panamint Valley fault zone to the southern Saline Valley fault zone, forming a combined range front and intermontane fault system approximately 160 km long (Fig. 2). The fault system is a component of the Eastern California shear zone that, at this same latitude, also includes the Death Valley–Furnace Creek–Fish Lake Valley and the Owens Valley–White Mountain fault systems. The Eastern California shear zone accommodates Pacific Plate motion which is not taken up by

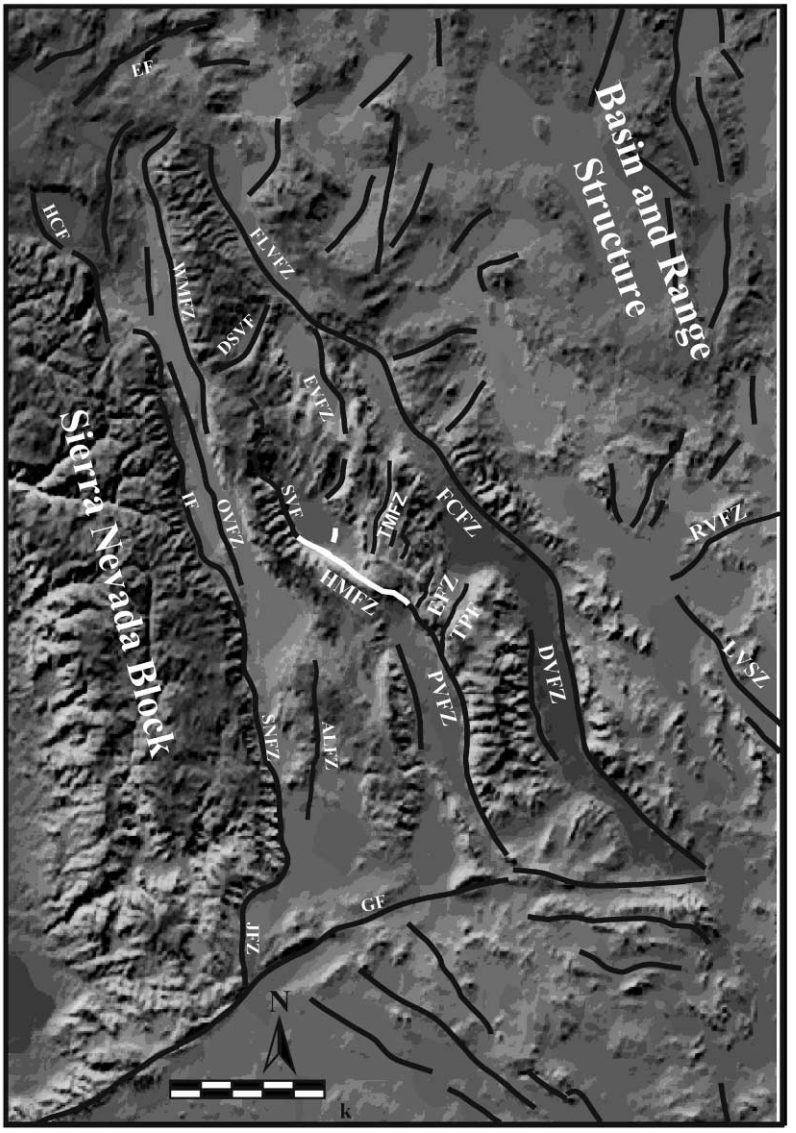

Fig. 2. Major faults and geographic features of the southern Walker Lane. The faults and shear zones are labelled as follows: Hunter Mountain (HMFZ, white), Garlock (GF), Jawbone (JFZ), Sierra Nevada (SNFZ), Airport Lake (ALFZ), Panamint Valley (PVFZ), Death Valley (DVFZ), Las Vegas (LVSZ), Townes Pass (TPF), Emigrant (EFZ), Independence (IF), Owens Valley (OVFZ), Saline Valley (SVF), Tin Mountain (TMFZ), Furnace Creek (FCFZ), Rock Valley (RVFZ), White Mountains (WMFZ), Deep Springs Valley (DSVF), Fish Lake Valley (FLV), Hilton Creek (HCF), and Excelsior (EF).

the San Andreas fault system west of the Sierra Nevada. Five normal fault zones, striking north to northeast, extend between the Panamint Valley–Hunter Mountain–Saline Valley fault system and the Furnace Creek and Fish Lake Valley faults. These faults include the Deep Springs Valley fault, the Eureka Valley fault zone, the Tin Mountain fault, the Townes Pass fault, and the Emigrant fault. All five faults are within the Inyo block of the southern Walker Lane and display some evidence for Quaternary offset along portions of their lengths (Beanland and Clark, 1994, dePolo, 1989; Sawyer,

1991; Reheis, 1991; Brogan et al., 1991; Smith, 1976; Zellmer, 1980; O'Malley, 1980). Hunter Mountain and the majority of the Nelson Range are comprised of the Hunter Mountain Batholith (McAllister, 1956; Hall and McKevitt, 1962). The Hunter Mountain Batholith is an approximately 500-km^2, early Jurassic, quartz monzonite intrusion exposed in the ranges to the east of the Sierra Nevada (Fig. 3; Dunne et al., 1978; Dunne, 1979; Chen and Moore, 1982). The maximum age for the development of northern Panamint Valley is at 4.0–4.3 Ma (Larson, 1979). Burchfiel et al. (1987) reported 8–10 km of post Late Cenozoic right-lateral offset of the Hunter Mountain Batholith along the Hunter Mountain Fault zone based on the offset of a piercing point. The piercing point is defined by the essentially vertical eastern wall of the Hunter Mountain Batholith and the basal unconformity with the overlying Miocene–Pliocene basalts (Fig. 3). The stratigraphy of dated volcanic flows was used by Larson (1979) to infer that Saline Valley was in existence by 3.1–1.8 Ma. Burchfiel et al. (1987) used maximum ages for the inception of Saline and northern Panamint Valleys to interpret a slip rate of 2.0–3.2 mm/year for the Hunter Mountain fault zone. Zhang et al. (1990) calculated a similar slip

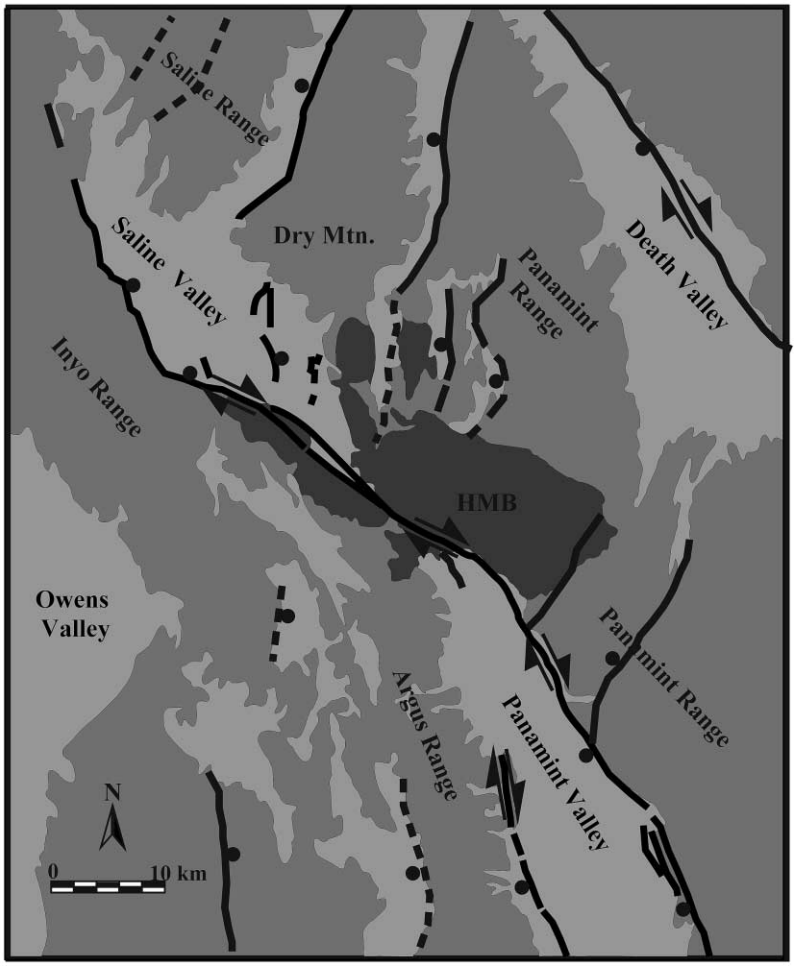

Fig. 3. Sketch map of the Hunter Mountain Batholith showing the 10 km of right-lateral offset along the Hunter Mountain fault zone. Valleys are light gray, ranges medium gray, and the Hunter Mountain Batholith is dark gray (modified from Burchfiel et al., 1987).

rate of 2.4 mm/year for the southern Panamint Valley based on the offset of geomorphic features on Quaternary alluvial surfaces.

The observation that northwest-trending, right-lateral faults in the western Great Basin and similar faults within California are "definitely related" was made by Gianella and Callaghan (1934) in their description of the 1932 Cedar Mountain earthquake. Subsequent to 1934, all efforts by researchers to quantify the rate of slip and to kinematically link slip within the Walker Lane Belt to Pacific Plate motions initiate from the original observations of Gianella and Callaghan, made some 36 years before modern plate tectonic theory was widely accepted. This observation set the stage for the definition of the Walker Line by Billingsley and Locke (1939), who later called it the Walker Lane (Locke et al., 1940). Stewart (1980) described the Walker Belt as a zone of diverse-trending topography that lies west of the Sierra Nevada and later used the term Walker Lane Belt after Carr (1984). The Walker Lane Belt sits between the Sierra Nevada block to the west and "typical" basin and range structure to the east (Stewart, 1988). More recently, the term Eastern California shear zone was used by Dokka and Travis (1990) to describe the entire set of right-lateral strike-slip faults that lie between the Sierra Nevada and the Great Basin from the big bend in the San Andreas Fault system northward into eastern Oregon and Washington (Pezzopane and Weldon, 1993; Wise, 1963; Bird and Rosenstock, 1984; Dokka and Travis, 1990; Sauber, 1990). Additionally, the faults of the Eastern California shear zone are proposed to accommodate about 1 cm/year of Pacific Plate motion not accounted for by slip along faults of the San Andreas system west of the Sierra Nevada (Atwater, 1970; Dokka and Travis, 1990; Ward, 1990). During the last two decades, researchers have used geodesy and very long baseline interferometry (VLBI) to begin defining the modern distribution of strain accumulation within this region (Savage and Lisowski, 1990, 1995; Savage et al., 1990; Dixon et al., 1995).

Currently, discrepancies exist between the interpretation of how the slip is distributed among the three fault systems. Differences are found between different geodetic models, and geodetic models and published geologic evidence. Savage et al. (1990) and Savage and Lisowski (1995) placed about 7–8 mm/year of dextral slip on the Owens Valley fault system; however, the authors admitted that because of the location of their VLBI stations all or some smaller portion of the slip could occur to the east of Owens Valley. By placing almost the entire slip budget for the Eastern California shear zone within Owens Valley, the model contradicts geologic evidence of a Holocene lateral slip rate of 2 ± 1 mm/year and an average slip rate of 1.5 ± 1 mm/year for Owens Valley (Beanland and Clark, 1994). The discrepancy becomes more salient if one also considers geologic evidence of a minimum slip rate for the Hunter Mountain fault zone of 2.6 ± 0.6 mm/year (Burchfiel et al., 1987) and a slip rate of 5–12 mm/year for the Furnace Creek fault zone (Klinger, 1994).

In contrast, Dokka and Travis (1990) proposed a kinematic model that suggests the approximately 10 mm/year of dextral shear across the Mojave Desert is transferred north of the Garlock fault primarily along the Death Valley–Furnace Creek and the Panamint Valley–Hunter Mountain fault systems. This model conflicts with the geologic and geodetic observations of Savage and Lisowski (1990, 1995) and Beanland and Clark (1994) that show the Owens Valley fault zone is slipping at about 2 mm/year.

Dixon et al. (1995) present a third model based on geodetic and geologic evidence that calls for an almost even distribution of Late Quaternary dextral slip between the three fault systems with 3.9 ± 1.1 mm/year on the Owens Valley fault system, 3.3 ± 2.2 mm/year on the Death Valley–Furnace Creek fault system, and the reported 2.6 ± 1 mm/year for the Panamint Valley–Hunter Mountain–Saline Valley fault system. The model of Dixon et al. (1995) suggests that present-day dextral slip is transferred north and eastward, from the Panamint Valley–Hunter Mountain and Owens Valley fault systems to the Fish Lake Valley fault zone, by means of northerly trending normal faults. Their model suggests that the Deep Springs Valley fault and the Eureka Valley fault system presently accommodate the transfer of slip onto the Fish Lake Valley fault system. At the latitude of the White Mountains and Fish Lake Valley fault zones, dextral slip is distributed 3.4 ± 1.2 mm/year and 6.2 ± 2.3 mm/year, respectively. Their model also attempts to rectify differences in the geodetic and geologic rates by suggesting rapid changes in the temporal and spatial distribution of dextral slip. In

this model, the distribution of slip on the northerly trending, active normal faults has migrated north and westward, with the northern transfer faults becoming more active as time progresses. Their model shows that the northerly trending normal faults within Saline Valley are active post 4 Ma. The time line correlates quite well with stratigraphic evidence of deformation on basalt flows in the Dry Range and the Saline Range suggesting the opening of Saline Valley occurred between 3.1 and 1.8 Ma (Larson, 1979). Within this window of time, northerly trending, normal faults within Saline Valley must be active along with northwest-striking, right-lateral, strike-slip faults to accommodate the opening of Saline Valley as a rhombochasm.

3. Methods

Mapping of fault zone and associated Quaternary deposits was conducted with 1:28,000 scale, color aerial photography in Saline Valley (Bureau of Land Management, CMOO series, 1975) and 1:10,000 scale, low-sun angle, black and white photography along the Hunter Mountain fault zone. Interpretive linework from the aerial photography was field verified and transferred to the U.S. Geological Survey orthophotoquads. Scarp heights and displacement amounts were calculated in the field using compass and pace techniques. The linework from the orthophotoquads was, in turn, transferred to the U.S. Geological Survey, 1:24,000 scale quadrangles. LAND-

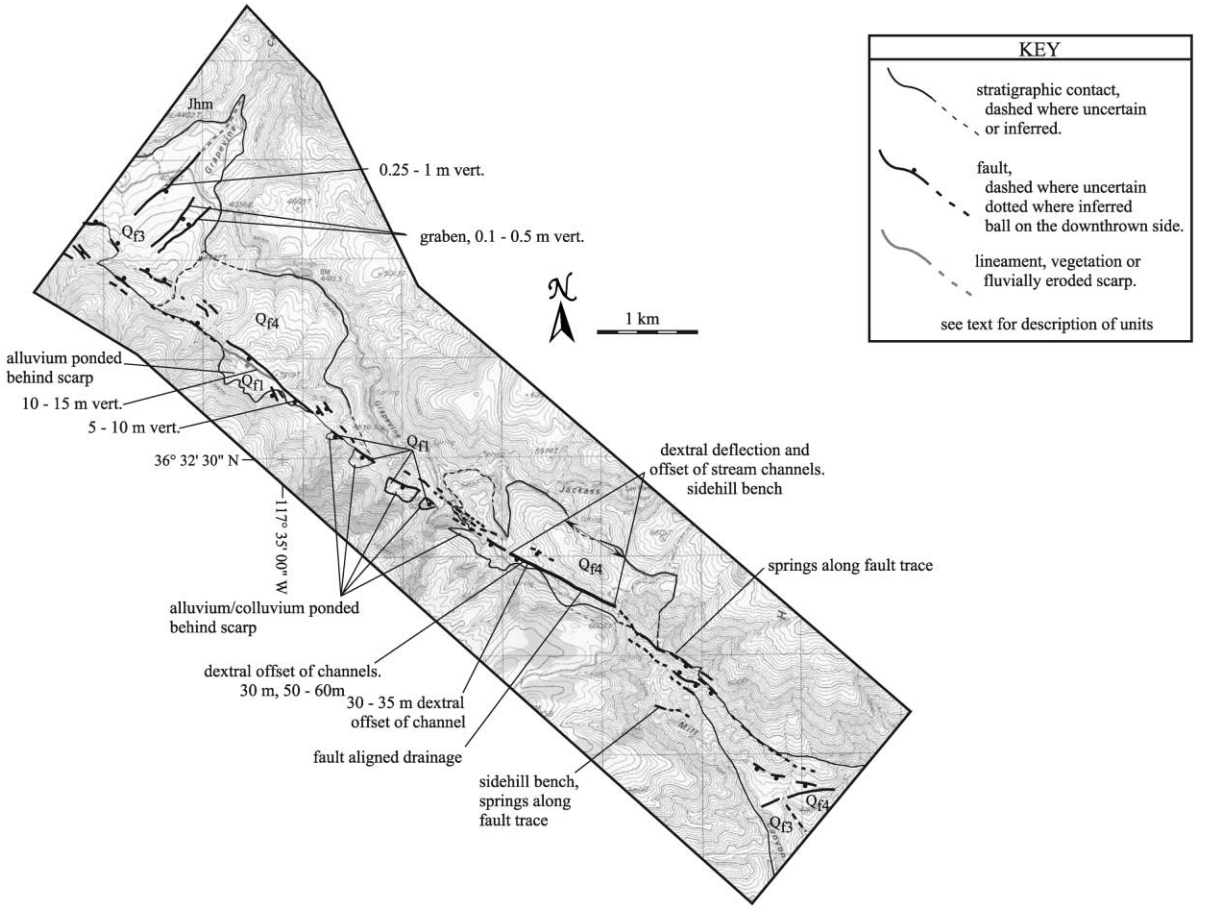

Fig. 4. Quaternary geology of the Hunter Mountain section showing the neotectonic character of faulting along the Hunter Mountain fault zone.

SAT Thematic Mapper (TM) imagery was used to check surface correlation in the more remote locations. The map was compiled on scanned images of the 1:24,000, USGS quadrangles reduced 50%, giving a 1:48,000 base (Oswald, 1998). The strip maps for this publication were taken from the 1:48,000 basemap (Figs. 4–8).

4. Results of mapping

4.1. Surficial geology

Map units are defined primarily on the basis of the degree of the development of surficial characteristics. Surficial characteristics have a relatively predictable range of features that are a function of the amount of time a surface is exposed to physical and chemical erosion. For example, fresh bar and swale morphology dominates the surface morphology of young alluvial fans; and, in turn, they are characterized by a sharp, rough appearance in aerial photography. Over time, the bar and swale morphology becomes muted by erosion of bar material infilling the swales. This process creates a smoother appearance to the older surfaces in aerial photography. As bar and swale morphology is muted, large areas of flat, pebble- to cobble-mantled pavement surfaces develop. The desert pavement areas become tightly packed with time, forming an armor over a flat surface. Development of desert varnish on exposed clasts causes the clasts to darken in color, making the older surfaces darker in aerial photography. The depth of dissection is greatest in the older surfaces, reflecting exposure to longer periods of channeling and fan entrenchment. Cross-cutting relationships require that younger alluvial units cut older units and are generally inset into older units. Description of the mapped units are the focus of this section. We then follow with a discussion of the interaction of the units with the Hunter Mountain fault zone.

4.1.1. Active surfaces

Qy, Qs, and Qd are the youngest allostratigraphic units mapped in the field area (Figs. 5 and 8). Qy describes modern channels or wash deposits that cut

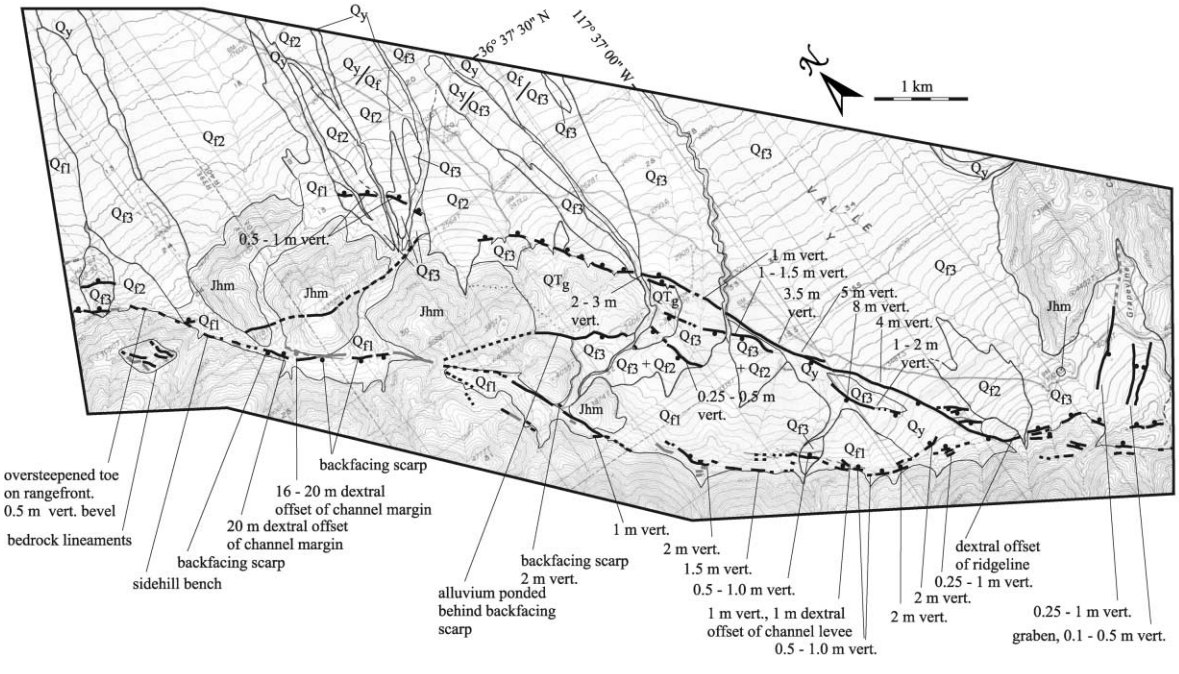

Fig. 5. Quaternary geology of the Nelson Range section showing the neotectonic character of faulting along the Hunter Mountain fault zone. Key as in Fig. 4.

or overlie all other surfaces. The Qy surface is readily distinguishable in aerial photography by its light, unvarnished color and rough appearance. On the ground, the Qy surface is characterized by fresh bar and swale morphology. The surface is nonvarnished and unpaved. Clasts are generally sub-rounded to sub-angular and can be up to 2–3 m in diameter. Soils generally are undeveloped or are poorly developed with weak Bk horizons. Based on the youthful soil and surface development characteristics, the Qy surface is presumed to be Latest Holocene to Modern in age.

Qd units are eolian sand dunes and sand drifts. Sand dunes are located to the east of the playa region and are characterized in aerial photography by their wind-sculptured forms and accumulation around vegetation. The dunes are oriented WNW to ESE, with the lee sides facing south. This orientation is transverse to the north to northwest prevailing wind. Transverse dunes are generally interpreted to be related to conditions of large sediment supply and ineffective winds (Bloom, 1978). In exposure, the dune sediments are well-sorted, well-rounded, fine to medium sand. Soils are undeveloped on active dunes and very weakly developed on vegetated, inactive dunes.

Qs marks more expansive, eolian sand sheets. The largest area of sand sheet deposits is the floor of Saline Valley. This unit is recognizable in aerial photography by a high albedo and a generally smooth, undissected appearance. In exposure, the unit is a rounded, fine- to medium-grained, silty sand that contains less than 20–30% of well-rounded, pebble- to cobble-sized clasts. The larger clasts generally occur within active channels in the Qs unit. A weakly developed to undeveloped Bk soil character-

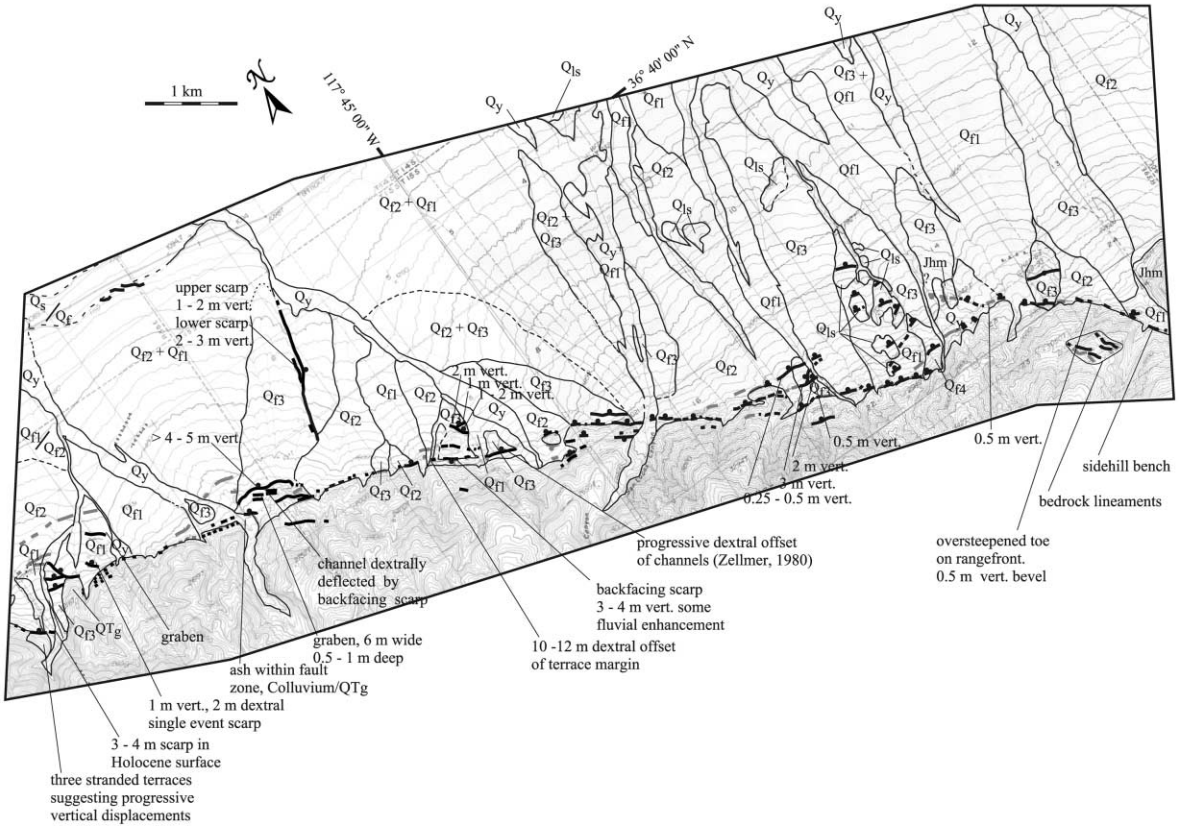

Fig. 6. Quaternary geology of the San Lucas Canyon section showing the neotectonic character of faulting along the Hunter Mountain fault zone. Key as in Fig. 4.

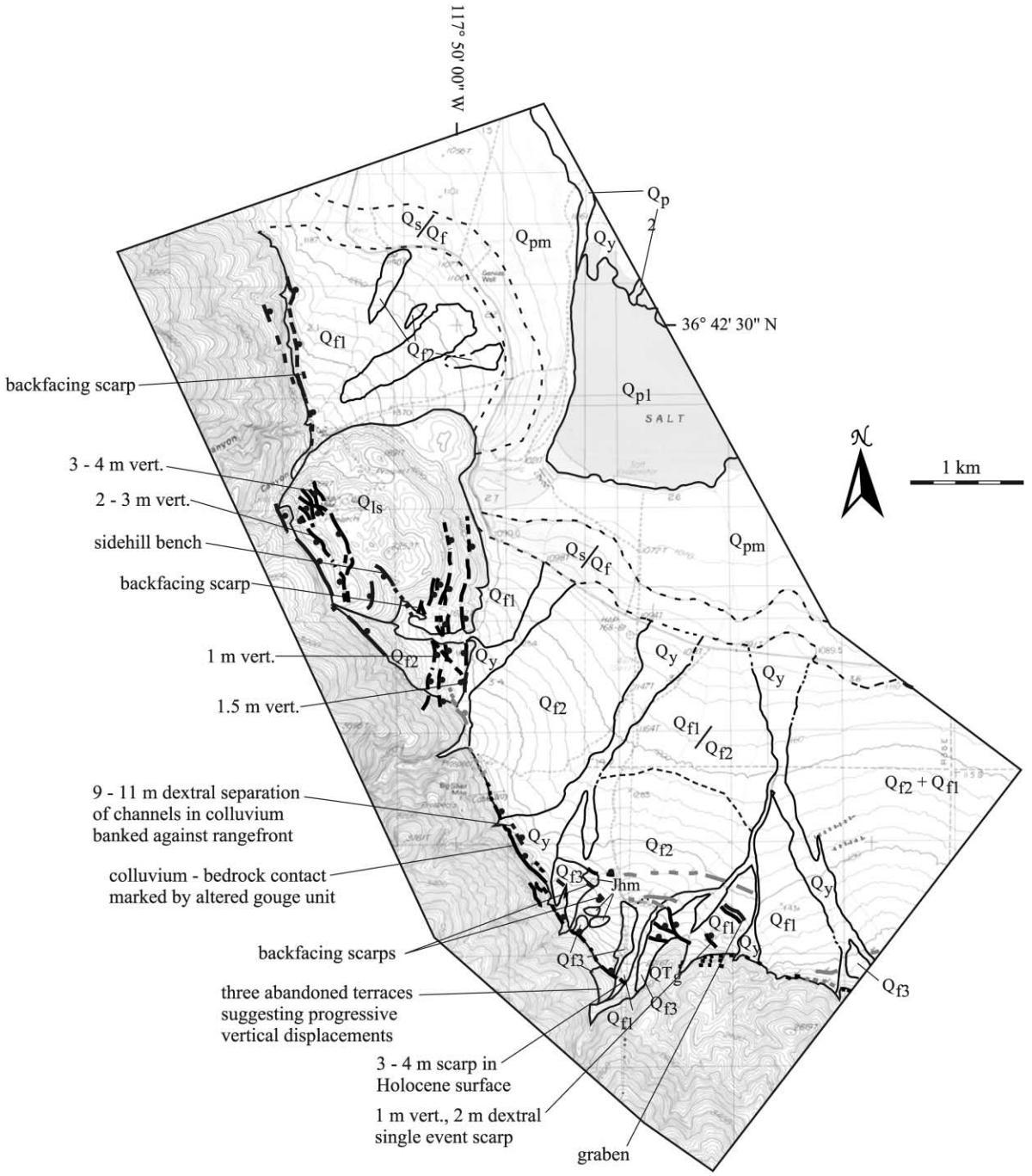

Fig. 7. Quaternary geology of the Inyo Mountains section showing the neotectonic character of faulting along the Hunter Mountain fault zone. Key as in Fig. 4.

izes the Qs surface. Qs is also used for a sand unit (Qs/Qf) mantling the toeslopes of alluvial fans surrounding the valley floor (Figs. 6–8). A high albedo and smooth appearance are characteristic of the Qs/Qf unit in aerial photography. This unit generally mutes the morphology of the underlying fan unit.

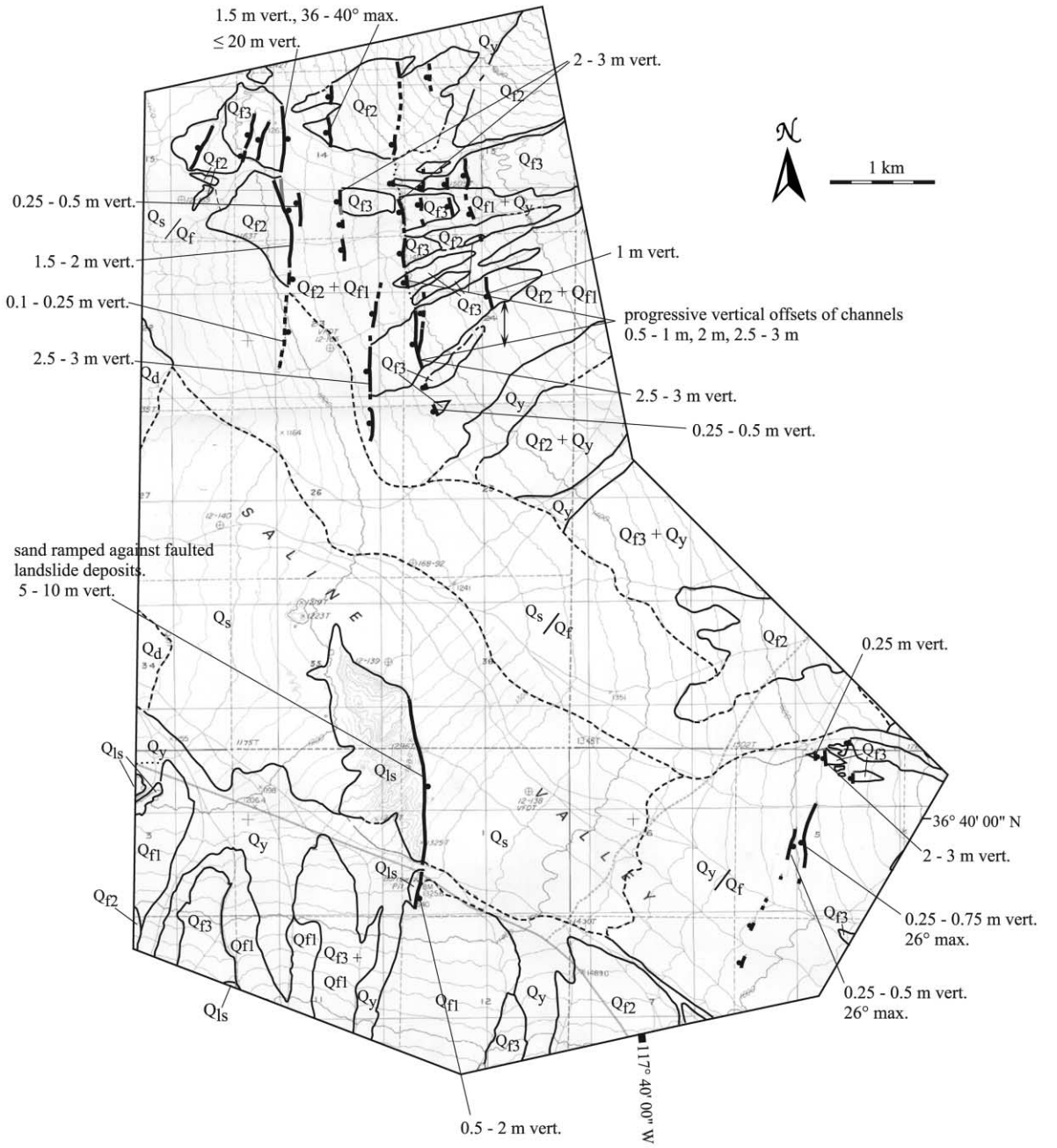

Fig. 8. Quaternary geology of the Saline Valley section showing the neotectonic character of faulting along the Hunter Mountain fault zone. Key as in Fig. 4.

The Qs/Qf unit is located around the entire floor of the valley, with the largest extent being on the predominantly downwind eastern side. Based on the distribution and depositional characteristics, we interpret the Qs/Qf unit as an eolian cap, locally derived from the playa and dunes of Saline and Owens Vallies.

4.1.2. Playa units

Qp1, Qpm, and Qp2 are playa allostratigraphic units. Previous detailed mapping of the saline deposits of Saline Valley by Lombardi (1957) assisted in the recognition of the three playa units mapped here.

The Qp1 surface is the lowest surface in the valley and is enclosed by the 325-m contour (Fig. 7). This unit is recognized in aerial photography by its extremely high albedo and flat, undissected appearance. In exposure, the playa surface has an almost pure salt crust underlain by a dark, clayey mud. The predominantly halite crust is formed by capillary efflorescence and is from 3 to 5 cm thick at the margin to 90 cm thick in the center of the playa (Hardie, 1968). The flat surface of the playa is controlled by the depth of the shallow water table and constitutes an active surface.

Qpm delineates playa margin mud and is recognizable in aerial photography as a dark apron along the playa margins (Fig. 7). The Qpm unit surrounds the playa, forming a dark, rough, blocky crust overlying fine-grained lacustrine mud and sands. The surface is dissected from runoff and channels entering the playa from the surrounding alluvial fans. The unit onlaps against the lower-most extents of fan surfaces at the playa margin. The playa mud unit is interpreted to have been deposited at a higher lake level. The distribution of unit Qpm along the western and southern edge of the playa suggests the lake may have been at least 2–3 m deeper in the past.

Adjacent and east of unit Qp1 is a second playa surface, Qp2 (Fig. 7). This unit is photogrametrically distinguishable from Qp1 by dissection of the playa surface from channels flowing from the eastern side of Saline Valley. In aerial photography, the unit is slightly darker in color than Qp1 because of a lack of a smooth crust. Qp2 is composed of fine lacustrine silts and clay with a blocky salt crust. The blocky texture of the crust is a result of salt heaving of the upper layers of silt during desiccation. The unit is contained within the 330-m contour and suggests lake depths of up to 5 m deeper are possible. An alternative scenario mentioned by Lombardi (1957) is the playa tilting westward as a result of faulting along the Inyo Range front. This scenario is supported by the occurrence of standing brine on the playa in the southwest against the range front and the deepening of the brine below the surface to the east (Lombardi, 1957). An approximately 5-m difference in elevation of the modern playa surface over a 9.5-km distance yields approximately 0.03° tilt to the west.

4.1.3. Alluvial fan units

Qf1, Qf2, Qf3, and Qf4 are alluvial allostratigraphic units. The Qf1 surface is the youngest alluvial surface mapped in the field area (Figs. 4–8). The Qf1 surface appears light colored, and rough textured in aerial photography. The unit is generally undissected to weakly dissected, although significant entrenchment of the fan head surface can occur where drainages leave the range front. In exposure, the Qf1 surface has fresh bar and swale morphology, undeveloped pavement, and weak to no varnish development. Soils are weakly developed, with weak stage I calcic soils. The youthful surface morphology and weakly developed soils suggest the Qf1 surface is Holocene in age.

The Qf2 surface is characterized in aerial photography by its light to medium brown, moderately dissected appearance. The texture of the surface is smoother in aerial photography than the texture of Qf1 surfaces. In exposure, the surface has moderately to well-developed varnish and has muted bar and swale to lobate-smooth morphology. Coarser, degraded bar regions separate swales with moderately to well-developed, patchy to stepped pavement sections developed within the swales. Stage II calcic soils with moderately developed cambic horizons distinguish soil development on Qf2 surfaces. Soil development on Qf2 surfaces suggests that they are Late Pleistocene in age.

Qf3 surfaces are distinguishable in aerial photography by a smooth, dark appearance and deep dissection. In exposure, the Qf3 unit has well-developed varnish and smooth, moderately to tightly packed, clast-supported, paved surfaces. The unit is deeply dissected. Soils are well-developed on Qf3 surfaces and generally obtain a stage III calcic soil.

The Qf4 unit is found in the southeastern corner of Saline Valley and within Grapevine and Mill Canyons. The unit is found in the higher elevations of the field area, making direct comparisons with the surficial characteristics of other units problematic. Where the Qf4 unit is adjacent to the Qf3 unit, the Qf4 grades to a significantly higher elevation than the Qf3. Equally problematic is the fact that the Qf4 unit represents many periods of terrace construction and dissection. Soils within the Qf4 unit generally have strongly developed stage III carbonate that engulfs a well- to moderately developed cambic horizon. Dissection of the unit ranges from one to tens of meters and represents many periods of dissection. We interpret the unit to represent an older alluvial/fluvial fill sequence deposited into the valley early in the development of modern Saline and Panamint Valleys. The older age for the Qf4 unit is supported by exposures in Grapevine Canyon of basaltic flows within and near the base of the unit. Geologic mapping within Grapevine Canyon suggests that one basaltic flow breached the Nelson Range near the pass between Saline and Panamint Vallies and flowed into Grapevine Canyon. Larson (1979) reports a 5.9 ± 0.2 Ma, K/Ar age of a basaltic flow on granite within Grapevine Canyon. K/Ar dates of other basaltic flows that rest on conglomerate within Saline Valley and the Panamint Range are less than 3 Ma (Larson, 1979). Because the basaltic flows are at the bottom of a thick package of gravels and the flows rest on gravels, we interpret the major surface that the Qf4 unit represents as early Quaternary in age. However, the many inset terraces within the unit are undoubtedly much younger and represent periods of stability between periods of dissection. The younger surfaces within the Qf4 unit are not differentiated due to scale and most likely span the Pleistocene and Holocene.

4.1.4. Landslide deposits

Unit Qls includes a group of remnant alluvial surfaces on the southwestern piedmont slope of Saline Valley, deposits within the center of Saline Valley, and surfaces built on a large range front block in the northwestern corner of the field area (Figs. 6–8). In aerial photography, the Qls units display a hummocky morphology characteristic of landslide deposits. The Qls surfaces on the southwestern piedmont slope are darkly varnished with smooth, tightly packed pavement. The surfaces are deeply eroded into individual remnants. In exposure, the unit is weakly to non-stratified and consists of angular to sub-angular clasts that are matrix to clast supported. Clast sizes range from 10 to 30 cm with clasts up to 2 m. In contrast to landslide deposits, fan units generally are well stratified, alternating between fluvial and colluvial modes of transport.

The Qls surface in the center of Saline Valley is characterized in aerial photography by a smooth, light-colored surface. A well-developed, cambic, stage III carbonate soil is developed in angular to sub-angular, clast- to matrix-supported gravels. Clast sizes range up to 1.5 m, with 10–25 cm being predominant. The light surface of the landslide unit observed in aerial photographs is due to the degraded granitic clasts and a thick eolian cap. Dark varnish is present where clasts are exposed and weakly degraded.

The Qls unit in the northwestern corner of the study area is an approximately 3-km^2 range front slide block of Paleozoic strata. Aerial photography reveals that the source area for the slide block is to the southwest and indicates approximately 2 km of displacement to the northeast. A 20–30-m vertical scarp along the western edge of the block forms the western edge of a graben complex that has formed since its deposition. The large displacement across the graben suggests a significant period of time has passed since deposition of the slide block. In outcrop, the slide block retains original stratigraphic layering. Closer inspection reveals the rock is not coherent but is broken into angular clasts.

4.1.5. Quaternary/tertiary fanglomerates

Unit QTg is comprised of the oldest alluvial sediments mapped within the field area (Figs. 5 and 6). The deposits are distinguished by being well above the modern grade. The QTg unit is characterized by well-indurated, sub-angular to rounded gravels. Alluvial gravels mapped as QTg in Grapevine Canyon contain tephra beds that dip up to 40°.

4.1.6. Jurassic granite

Unit Jhm is igneous intrusive quartz monzonite that comprises the Hunter Mountain Batholith. The unit is only mapped where surrounded by Quaternary sediments.

Table 1
Age divisions of the Quaternary

Age	Time span
Holocene (Qf1, Qy)	Historic–10 ka
late Pleistocene (Qf2)	10–128 ka
middle Pleistocene (Qf3)	128–738 ka
early Pleistocene (Qf4)	738–1600 ka

4.2. Age of units

Only unit Qf3 has an independent and quantitative age. A volcanic tephra found in a wash cut on the southwestern range front of Saline Valley correlates with the Glass Mountain ash bed of Death Valley (Sarna-Wojicki, personel communication, 1997). The tephra is reported to be 0.8–1.2 Ma and is found about 2 m down in a Qf3 surface. Based on the tephra, the degree of soil development, and surface morphology, we interpret the Qf3 surface to be Middle Pleistocene in age. With this constraint, we assume approximate age boundaries to the mapped Quaternary units based on the quantitative subdivisions of the Quaternary period put forth by Harland et al. (1990), Wesling et al. (1992), and Menges et al. (1996) (Table 1). Although the ages are approximate, they are sufficient to place broad limits on the rate and recurrence of fault motion when surfaces are displaced by the fault.

4.3. Rate and style of faulting

For the purposes of description, we divided the Hunter Mountain fault zone into five sections (Fig. 9). The sections are differentiated by changes in charac-

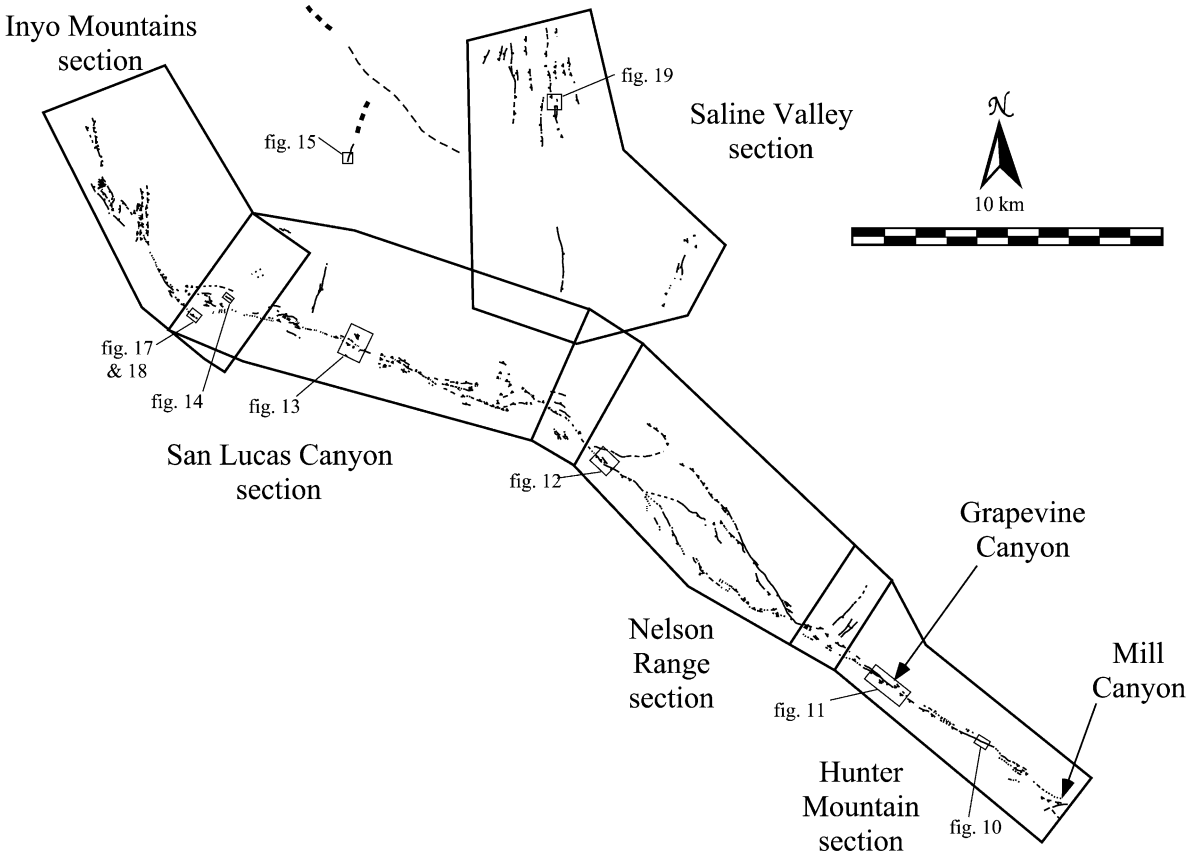

Fig. 9. Sections of the Hunter Mountain fault zone used for description of the characteristics of faulting and map figures. Locations of subsequent photographs are shown.

teristics of faulting along the fault trace, such as strike and sense of displacement.

4.3.1. Hunter mountain section

The Hunter Mountain section corresponds to an approximately 10-km section of the fault that trends N 50–60° W between Panamint and Saline Valleys (Figs. 4 and 9). The section is characterized by deep incision of drainages into Qf4 and Qf3 units. Localized aggradation of young alluvium is found behind back-facing (uphill-facing) scarps. Mill Canyon is aggressively eroding headward and northward into Grapevine Canyon. The stratigraphy is well-exposed in the deeply dissected Grapevine Canyon. Tephra found in alluvial/fluvial gravels of the Qf4 unit dip at up to 42° northeast along the fault zone.

Uppermost Grapevine Canyon is fault aligned, with the fault forming a sidehill bench along the north side of the upper 2 km of the canyon. Numerous perpendicular tributaries are dextrally deflected or offset across the fault trace, with one tributary showing a separation of 50–60 m (Fig. 10). The large dextral separations of drainages along this section of the fault display a history of repeated right-lateral offsets. Surficial characteristics and soil profiles revealed in wash cuts along the sidehill bench suggest that the surface of the sidehill bench is much younger than the deposit in which it is constructed. Surface clasts are fresh and relatively unweathered, and soil profiles exposed in wash cuts are weakly developed. Additionally, the pattern of closely spaced, short tributaries suggests that the dissection of the surface is occurring rapidly and is a relatively recent event. Research in Death Valley has suggested that the formation of alluvial fan surfaces occurs during times of climatic change (Wells et al., 1984, 1987). Material for these fan surfaces is derived from fan surfaces that are already in place or from alluvium within the ranges above the valleys. Upper Grapevine Canyon falls into the latter of the two environments. A significant climatic change from wet to dry occurred in the Latest Pleistocene, approximately 15 ka (Smith,

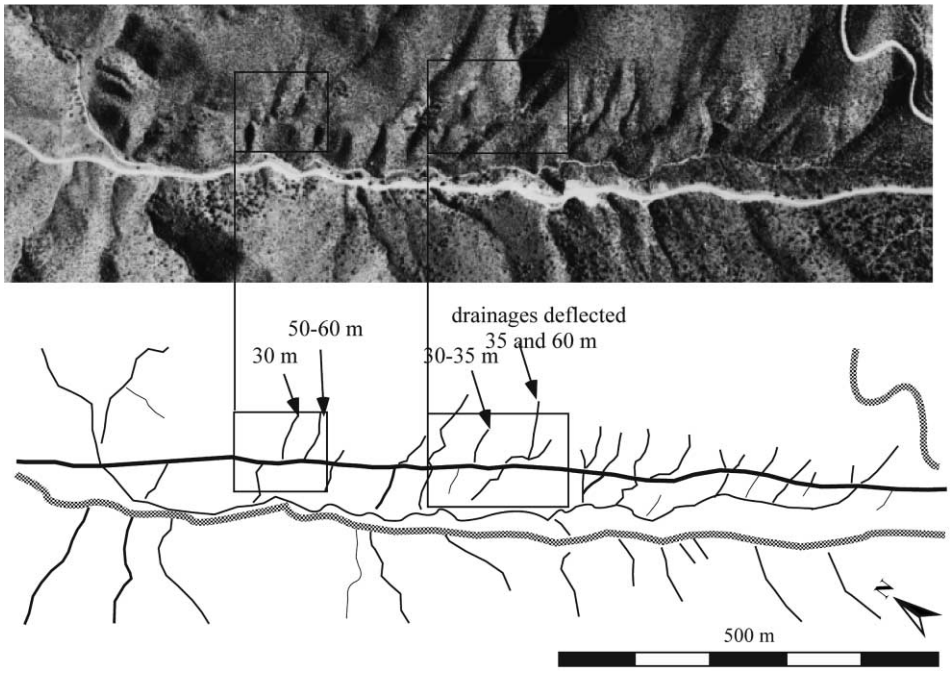

Fig. 10. Aerial photograph and sketchmap of drainage patterns near the pass between Panamint (to the southeast) and Saline (to the northwest) Valleys. Drainages are shown by the thin lines, the fault by the thick line, and the road by the gray line. Selected offset or deflected drainages are highlighted by the box and the separation noted.

1976; Howe and Lowenstein, 1996). Following this line of reasoning, we suggest that the recent incision in Grapevine Canyon occurred at this time, and offsets of this surface by the fault can yield an estimate of the Late Pleistocene slip rate. Using the maximum offset of drainages of 50–60 m, and assuming the age of the surface is 15,000 years, results in an estimated lateral slip rate of 3.3–4.0 mm/year.

Continuing southward, the fault crosses Grapevine Canyon about 2 km from the pass, forming a sidehill bench and back-facing scarps on the south side of the canyon (Fig. 11). Youthful alluvium is ponded behind back-facing scarps that have up to 15 m of vertical separation. A series of two left-stepping traces dextrally deflects a drainage 32 m around a back-facing scarp. A second drainage to the north is deflected by a back-facing scarp approximately 60 m in a right-lateral sense. Thus, in summary, the morphology of the fault zone indicates that motion is principally strike-slip, and observations are consistent with late Quaternary motion along the fault zone.

Although the fault is primarily strike-slip, at the northern end of the Hunter Mountain section a graben and a normal fault trend approximately N 45° E. This orientation is almost 90° from the trend of the Hunter Mountain fault zone (Fig. 9). The normal fault produces less than 1 m of vertical offsets of the Middle Pleistocene Qf3 unit and thus appears less active than the main trace or relatively young.

4.3.2. Nelson Range section

The Nelson Range section is 10 km in length, trends more northerly than sections to the north and

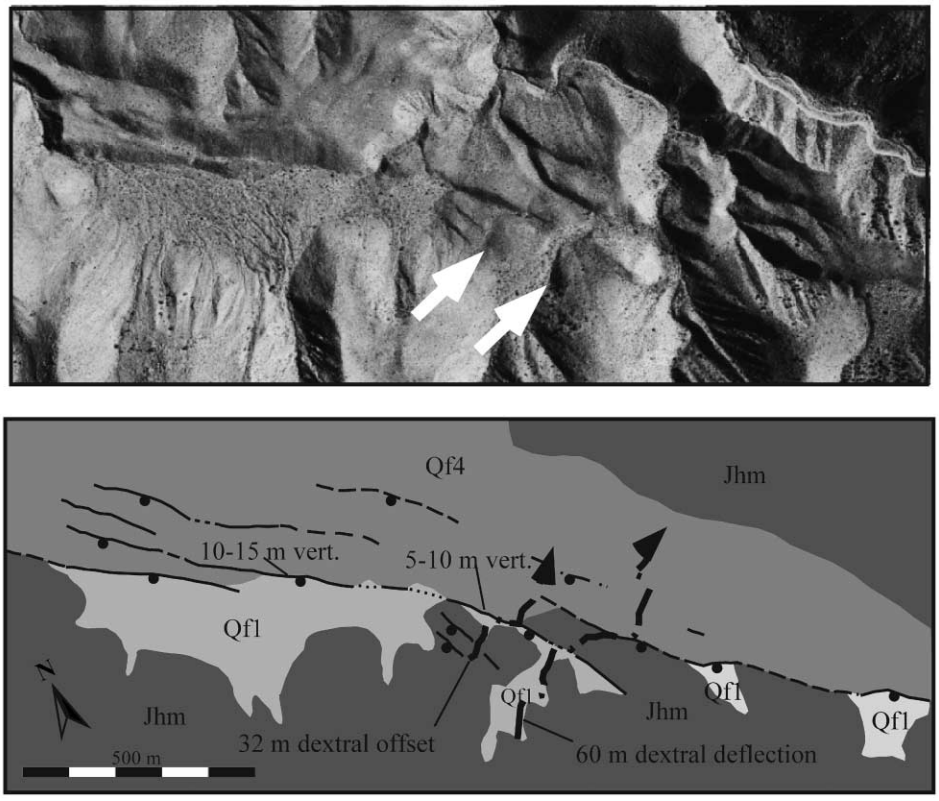

Fig. 11. Aerial photograph and geologic map of location in the Hunter Mountain section where Holocene sediments are ponded behind back-facing scarps that deflect drainages in a dextral sense. Drainages are the dash-dot line. Arrow shows direction of flow. Faults are the heavy black lines, ball is on the down-thrown side. Contacts are the thin black lines. The northern drainage is deflected approximately 60 m. The southern drainage is deflected 32 m.

south, and marks where the fault first enters Saline Valley. Additionally, it is marked by a large graben along its length and a range front that is steeper than sections immediately to the north and south (Figs. 5 and 9). The faulting geometry and range front morphology are consistent with an increased normal component of motion being manifest in a broad 1.5-km right step between the sections to the north and south, which are principally strike-slip. A dextral component of motion is also indicated by the left-stepping nature of the range-bounding portion of the fault and the preservation of an abandoned drainage on a Holocene surface showing 1 m of dextral separation (Fig. 5). Also, north of the graben, a

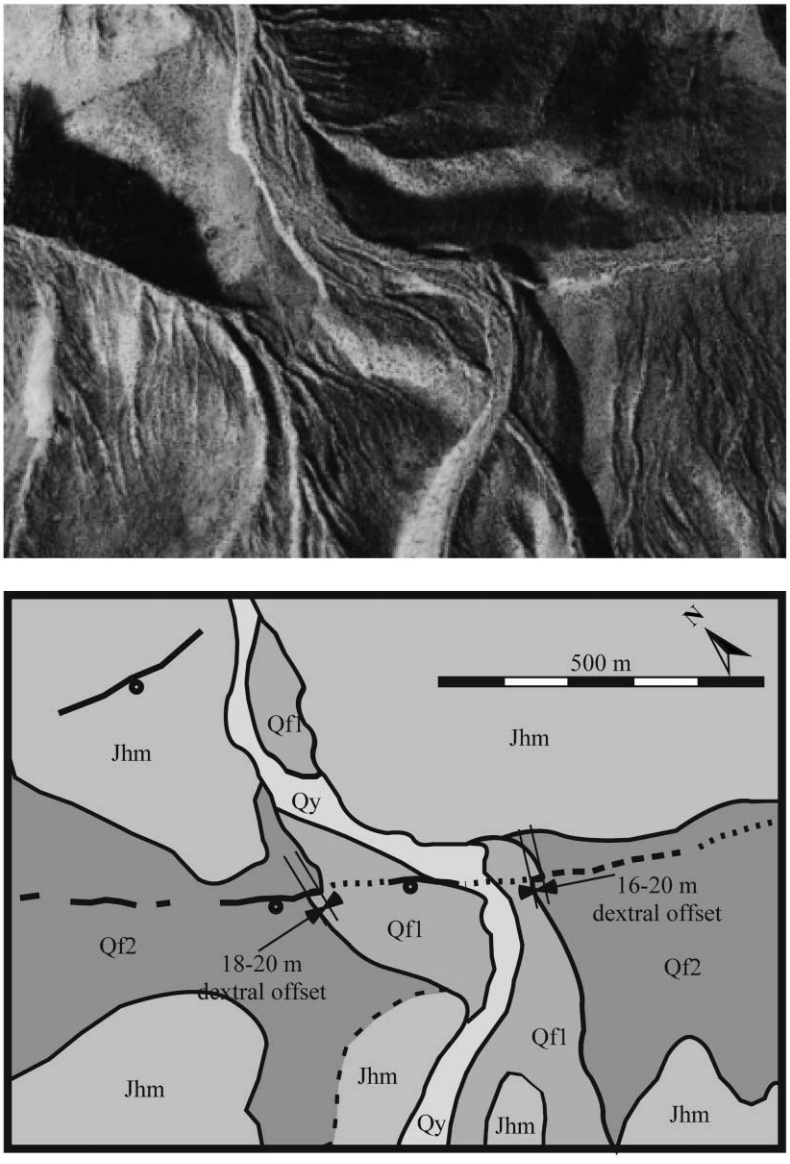

Fig. 12. Aerial photograph and geologic map of an offset channel margin. Located in the Nelson Range section. Approximate amount of dextral offset is shown by the scale bars. Map symbols same as in Fig. 6.

channel margin that is incised 2–3 m into a Holocene Qf2 surface is dextrally offset 16–20 m (Figs. 5 and 12). Dividing the offset by the limits of the age of the Qf2 surface yields a broad minimum on the lateral slip rate of the fault between 0.125 and 2.0 mm/year. The rate is a minimum in the sense that offset of the incised channel postdates formation of the surface into which it is incised.

4.3.3. San Lucas Canyon section

The *San Lucas Canyon section* is approximately 12 km in length and trends more northwesterly than the Nelson Range section to the south (Figs. 6 and 9). The range front within this section is generally more laid back, as opposed to the more precipitous sections immediately to the north and south. The difference in range front morphology appears to be a direct result of differences in the predominant slip vector along the fault sections.

Laterally offset geomorphic features are not commonly preserved in the San Lucas Canyon section. However, lateral displacement is suggested by the offset and isolation of progressively older fan surfaces and drainages on the hanging wall block to the south of canyon mouths as the fault slips, while the drainage maintains a channel oriented perpendicular to the range. The pattern is illustrated outboard of an unnamed canyon just to the west of San Lucas Canyon (Fig. 13). In Fig. 13, the surfaces to the south of the canyon mouth marked by the white arrow become progressively older to the south. The age progression is probably the result of continued right-lateral offset along the fault, resulting in isolation of progressively older fan remnants to the south of the canyon mouth. Additional evidence for right-lateral faulting in Fig. 13 is a 10–12 m dextral offset of the terrace edge marked by the black arrow. The recency of faulting is displayed by a 1-m scarp crossing the Late Pleistocene Qf2 surface to the north and a lineament that crosses into the Holocene Qf1 surface. At the very northern end of the San Lucas Canyon section, there also exists a single-event scarp that offsets a Holocene fan surface by 1 m vertically and 2 m dextrally (Figs. 6 and 14). From the similarity of the size and style of Holocene single-event offsets along the Nelson and Inyo sec-

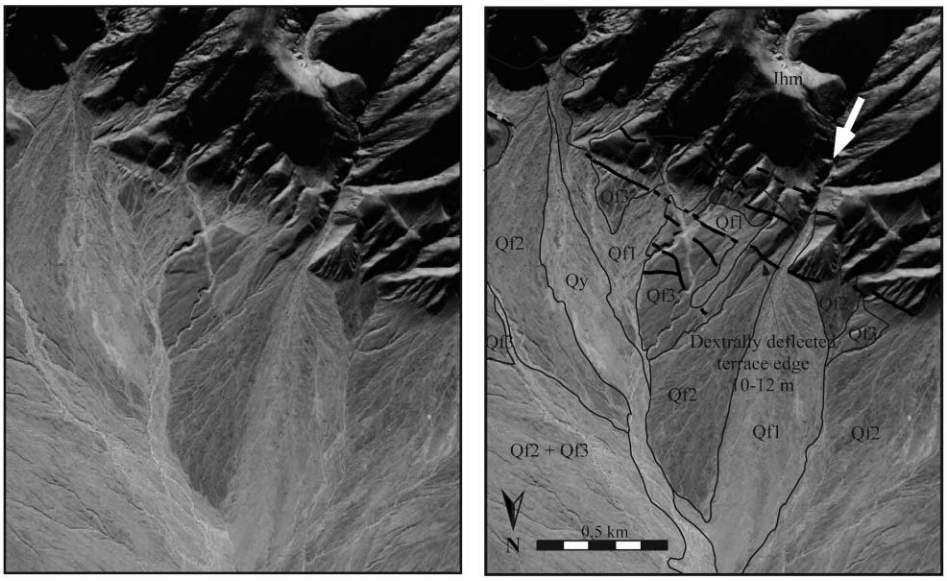

Fig. 13. Aerial photograph and geologic map of a location in the San Lucas section that demonstrates the process of isolating and preserving of fan remnants to the south of canyon mouths during continued right-lateral slip on the fault. The surfaces to the south of the canyon mouth marked by the white arrow become progressively older to the south. Additional evidence for right-lateral faulting is the 10–12-m dextral offset of the terrace edge marked by the black arrow.

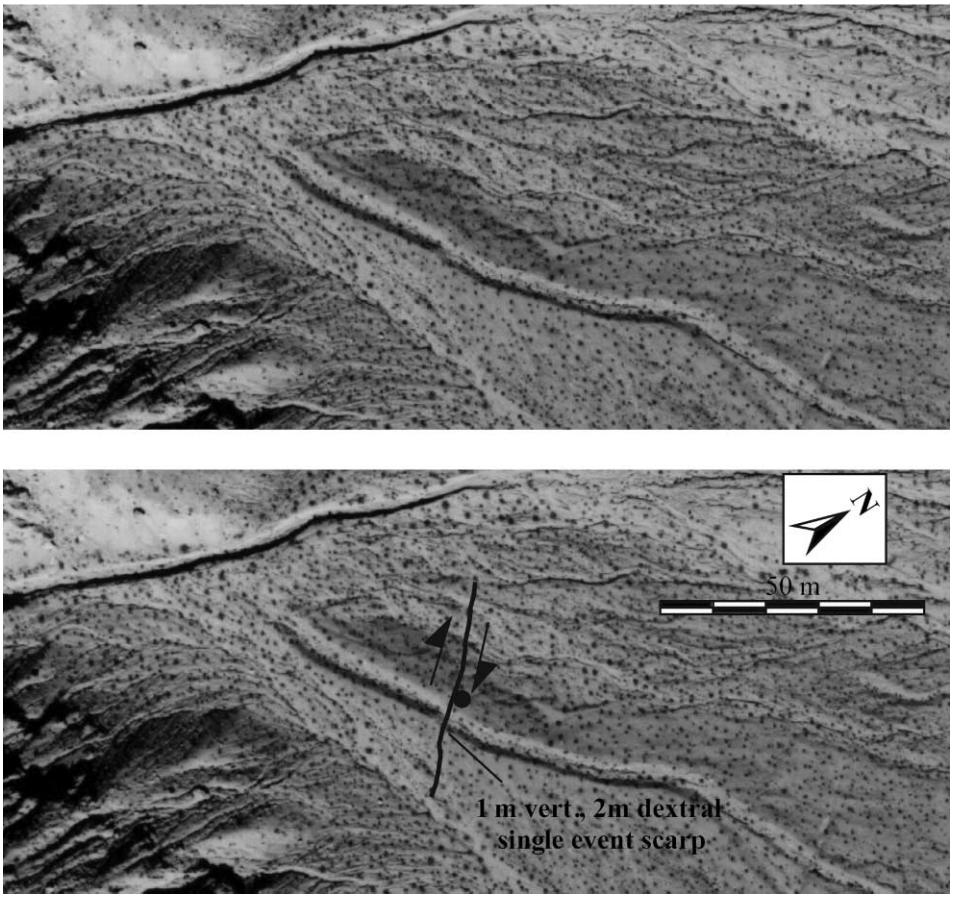

Fig. 14. Aerial photograph and interpretation of a lateral offset of a levee in a Holocene surface. The levee is offset 2 m dextrally, and 1 m vertically. Arrows show the sense of motion, and the ball is on the down-thrown side of the fault. The scarp is partially scoured and buried adjacent to varnished surface where offset is apparent.

tions, we suggest that both sections may rupture simultaneously.

Also at the northern end of the San Lucas Canyon section, a single normal fault trends almost 90° to the Hunter Mountain fault zone (Fig. 6). The scarp displays about 2–3 m of vertical separation of a Qf3 surface, ending at a young drainage on the northern end. On strike and approximately 3.5 km to the north, another normal fault displays a 10–15-cm down-to-the-east scarp that crosses the late Pleistocene to Holocene playa surface Qp2 (Fig. 15). The scarp trends north to northeast for almost a kilometer and ends at an active drainage dissected into the Qp2 playa surface. The preservation of the small scarp within the playa surface seems indicative of a late Holocene, if not historical, event.

4.3.4. Inyo Mountains section

The *Inyo Mountains section* encompasses the northernmost mapped portion of the range front fault zone. The section trends more northerly than the San Lucas section just to the south and is the southern end of the Saline Valley fault (Figs. 7 and 9). The range front displays morphology that is classically associated with normal faulting. Large triangular facets and wine-glass canyons dominate the steep range front (Fig. 16). The most recent displacement is recorded at the mouth of Daisy Canyon where a 3-to 4-m vertical

Fig. 15. Small scarp crossing a playa surface. The pen in the scarp gives scale.

scarp breaks a Holocene terrace surface (Fig. 17). The offset surface has fresh bar and swale morphology, very little to no pavement or varnish development, and a weak stage I carbonate soil. The sharp, planar nature of the scarp and lack of any bevels suggests that the scarp is the result of a single earthquake. The repeated occurrence of earthquakes through the late Pleistocene is preserved in a series of uplifted terraces adjacent to the mouth of Daisy Canyon (Fig. 18). Elsewhere along the range front, the fault zone is generally manifest as a bedrock colluvium contact, leaving little evidence for the recency of faulting.

Fig. 16. The range front along the Inyo Mountains section, showing steep triangular facets, wine-glass canyons, and a bedrock-colluvium fault trace characteristic of normal faulted range fronts.

Fig. 17. A 3–4-m scarp at the mouth of Daisy Canyon along the Inyo Mountains section. The scarp, in shadow, crosses the center of the photograph and offsets a Holocene surface. The offset surface displays fresh bar and swale morphology characteristic of a Holocene surface.

A large slump block at the northern end of the study area is cut by a complex graben system (Fig. 7). The faults cut all alluvial surfaces on the block except the most recent drainages. Vertical separations across individual strands of the fault are up to 3–4 m. The scarps are generally at the angle of repose, have sharp crests with occasional free faces, and lack any bevels, all of which suggest the scarps are the result of a single Holocene event. The continuity of the fault zone across the slump block with the bedrock-allu-

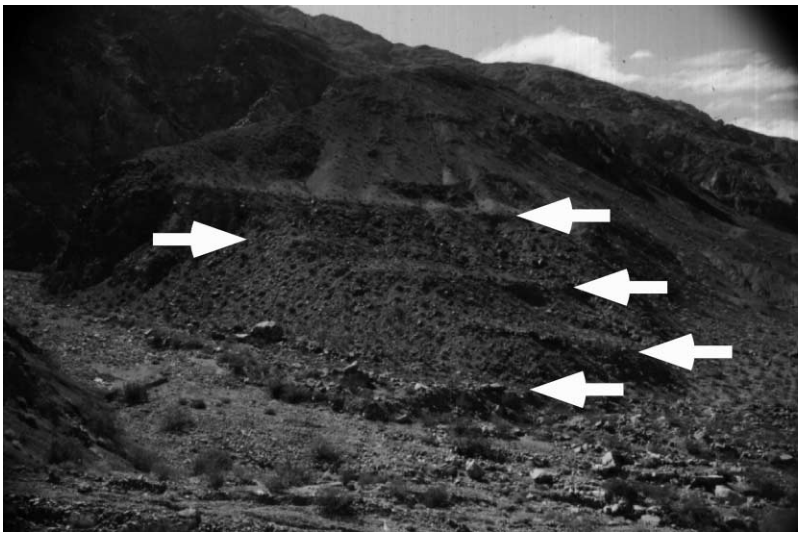

Fig. 18. Progressive flight of alluvial terraces preserved tens of meters above current stream grade indicate repeated normal displacements through late Quaternary time at this location. White arrows delineate the terrace risers. Scarp in Fig. 17 is the lowest arrow on the right.

Fig. 19. Progressively greater fault displacements are recorded on progressively older surfaces along the east-bounding graben scarp of the Saline Valley section. A 3-m scarp, which trends south away from photographer, is recorded on a Qf3 surface. Two inset surfaces show smaller scarps and, hence, record younger displacements. Youngest and smallest vertical separation (0.5 m) recorded by scarp is immediately left of Kimberly. An intermediate age displacement (2-m vertical separation) is recorded on surface just visible at bottom left of photo.

vium traces to the north and south, combined with the youthful nature of the scarps, lead us to suggest that the scarps here reflect the same Holocene offset as recorded at Daisy Canyon.

4.3.5. Saline Valley section

The *Saline Valley section*, in contrast to the previous range front sections, trends across the piedmont. The fault system is characterized by a fault graben that is oriented almost 90° from the range front sections of the Hunter Mountain fault zone (Figs. 8 and 9). The graben trends toward a NNE-trending valley that links Saline Valley with Eureka Valley (Fig. 2). Offsets within the Saline Valley section show normal separations, and surfaces show progressively greater vertical separations across respectively older surfaces. Up to 20 m of vertical separation is registered on the oldest Qf3 unit on the west-bounding fault of the graben. The eastern wall of the graben is formed by three or four fault strands, showing up to 3 m of vertical separation. Faults along both margins cut Holocene fan surfaces to the south. Clear evidence for at least three displacements is found along the main east-bounding scarp of the graben (Fig. 19). To summarize, the graben system records at least three events since middle Pleistocene. The western margin of the graben has up to 20 m of separation on the middle Pleistocene Qf3 surface. The eastern margin of the graben displays a total vertical separation on the same Qf3 surface of up to 7–9 m. The total separation across the graben system is about 11 m. The 11 m total separation of the Qf3 surface can be explained by a slip rate on the order of 0.02 mm/year. However, using the age of the surface to determine the slip rate requires that the rate be considered a minimum.

5. Discussion and conclusion

Our mapping of the Hunter Mountain fault zone clarifies the Holocene and right-lateral nature of slip along the Hunter Mountain fault zone. Within Grapevine Canyon, the fault shows primarily right-lateral motion within an intermontane valley. As the range front fault traverses northward into Saline Valley, the fault acquires a component of normal motion in addition to the strike-slip. Within the valley, those sections of the fault striking more northerly show a range front morphology consistent with an increased component of normal slip.

Displacement of Quaternary surfaces by the fault allows us to place a broad limit on the minimum lateral component of the fault slip rate. Within Grapevine Canyon, offsets of drainages incised into alluvium that we interpret to be Holocene to latest Pleistocene in age are used to place an estimate of the fault slip rate at between 3.3 and 4.0 mm/year. The Quaternary rate is slightly larger than the 2.0–3.2 mm/year slip rate reported for the fault by Burchfiel et al. (1987) on the basis of a 3 to 4 million-year-old piercing point. However, the similarity of the values is consistent with the idea that the slip rate has been relatively constant since inception of the fault.

The occurrence of displacement of Holocene deposits shows the recency of deformation and is suggestive of a relatively frequent earthquake return time. An approximate estimate of the average return time of earthquakes can be made if we use the displacements recorded on single-event scarps. Within Saline Valley, the best recorded single-event scarps are preserved displacements of Holocene debris flow levees (e.g., Fig. 14) and range from 1.5 to 2.5 m. Dividing the range of offsets by the 3.3–4.0 mm/year slip rate determined in Grapevine Canyon yields would place the return time of similar sized events between 375 and 860 years. The relatively short recurrence time appears consistent with the flight of young abandoned alluvial terraces preserved adjacent to Daisy Canyon (Fig. 18) as well as the abrupt and steep morphology of the Saline Valley range front (Fig. 16).

The Hunter Mountain–Saline Valley Fault system terminates along northeast-striking normal faults within the Saline Range. Reheis et al. (1996) suggest these normal faults transfer right-lateral slip eastward to the Furnace Creek–Fish Lake Valley fault zone. Our observations of small normal faults splaying northward off the main strike-slip trace and within Saline Valley support interpretations by Reheis and Dixon (1996) and show the mechanism to be active at the latitude of our study area.

Our observations show that the Hunter Mountain fault zone is a major and active structural element accommodating shear within the Walker Lane. Because the fault shows principally strike-slip motion along its southeastern reach, we can use the strike of the fault (N 55 °W) to locally define the azimuth of maximum shear accommodation. The azimuth is significantly more westerly than other major strike-slip faults within the Walker Lane, such as the Owens Valley (N 10–30° W) and Furnace Creek (N 30° W) faults (Fig. 2). The direction of maximum shear strain accumulation measured geodetically is also significantly more northerly than the strike of the Hunter Mountain fault zone. For example, Dixon et al. (1995) use Satellite Laser Ranging and VLBI to show that the displacement of the Sierra Nevada with respect to North America is N 38 °W and the motion of Sierra Nevada with respect to Ely is N 9 °W. The geodetic results imply a significant component of thrust motion along the Hunter Mountain fault zone, whereas our observations show a predominantly dextral strike-slip component. One may infer from these observations that, while geodetic measurements may accurately measure average rates and styles of strain accumulation across the Walker Lane, significant uncertainty remains concerning the relationship of the pattern of strain accumulation measured by geodesy to the pattern of strain release as manifest by slip on active faults.

Acknowledgements

Research was funded in part by National Science Foundation Grant EAR-93-04066. Center for Neotectonic Studies Contribution Number 37. Special thanks go to those who dared the summer temperatures of Saline Valley to assist in field work: Kimberly Oswald, Alan Ramelli and Giovanni Vadurro.

References

Atwater, T., 1970. Implications of plate tectonics for the Cenozoic evolution of western North America. Geol. Soc. Am. Bull. 81, 3513–3536.

Beanland, S., Clark, M.M., 1994. The Owens Valley fault zone, eastern California, and surface faulting associated with the 1872 earthquake. U.S. Geol. Surv. Bull. 1982, 29.

Billingsley, P., Locke, A., 1939. Structure of Ore Districts in the Continental Framework. Am. Inst. Mining Metall. Eng., New York, 51 pp.

Bird, P., Rosenstock, R.W., 1984. Kinematics of present crust and mantle flow in southern California. Geol. Soc. Am. Bull. 95, 946–957.

Bloom, A.L., 1978. Geomorphology: A Systematic Analysis of Late Cenozoic Landforms. Prentice-Hall, New Jersey.

Brogan, G.E., Kellogg, K.S., Slemmons, D.B., Terhune, C.L., 1991.

Late quaternary faulting along the Death Valley–Furnace Creek fault system, California and Nevada. U.S. Geol. Surv. Bull., 23 pp.

Burchfiel, B.C., Hodges, K.V., Royden, L.H., 1987. Geology of Panamint Valley–Saline Valley pull-apart system, California: palinspastic evidence for low-angle geometry of a Neogene range-bounding fault. J. Geophys. Res. 92, 10422–10426.

Carr, W.J., 1984. Timing and style of tectonism and localization of volcanism in the Walker Lane belt of southwestern Nevada. Geol. Soc. Am. Abstr. Programs 16, 464.

Chen, J.H., Moore, J.G., 1982. Uranium–lead isotopic ages from the Sierra Nevada Batholith, California. J. Geophys. Res. 87, 4761–4784.

DeMets, C., Gordon, R.G., Argus, D.F., Stein, S., 1990. Current plate motions. Geophys. J. Int. 101, 425–478.

dePolo, C.M., 1989. Seismotectonics of the White Mountains fault system, east-central California and West central Nevada. M.S. thesis, Reno, University of Nevada, Reno.

Dixon, T.H., Robaudo, S., Lee, J., Reheis, M.C., 1995. Constraints on present-day Basin and Range deformation from space geodesy. Tectonics 14, 755–772.

Dokka, R.K., Travis, C.J., 1990. Late Cenozoic strike-slip faulting in the Mojave Desert. Tectonics 9, 305–340.

Dunne, G.C., 1979. Hunter Mountain Batholith: a large, composite alkalic intrusion of Jurassic age in eastern California. Geol. Soc. Am. Abstr. Programs 11, 76.

Dunne, G.C., Gulliver, R.M., Sylvester, A.G., 1978. Mesozoic evolution of rocks of the White, Inyo, Argus, and Slate Ranges, eastern California. In: Howell, D.G., McDougall, K.A. (Eds.), Mesozoic Paleogeography of the Western United States. Pac. Coast Paleogeogr. Symp., vol. 2. Society of Economic Paleontologists and Mineralogists, Los Angeles, California, Pacific Section, pp. 189–208.

Gianella, V.P., Callaghan, E., 1934. The Cedar Mountain, Nevada, earthquake of December 20, 1932. Bull. Seismol. Soc. Am. 24, 345–377.

Hall, W.E., McKevitt Jr., E.N.M., 1962. Geology and ore deposits of the Darwin Quadrangle, Inyo County, California. U.S. Geol. Surv. Prof. Pap. 368, 87 pp.

Hardie, L.A., 1968. The origin of the Recent non-marine evaporite deposit of Saline Valley, Inyo County, California. Geochim. Cosmochim. Acta 32, 1279–1301.

Harland, W.B., Armstrong, R.L., Cox, A.V., Craig, L.E., Smith, A.G., Smith, D.G., 1990. A Geologic Time Scale 1989. Cambridge Univ. Press, New York, 263 pp.

Howe, L.K., Lowenstein, T.K., 1996. 150 ka paleoclimate history and chemical evolution of evaporites, Saline Valley, California. Geol. Soc. Am. Abstr. Programs 28, A-457.

Klinger, R.E., 1994. Late quaternary slip on the Death Valley and Furnace Creek faults, Death Valley, California. Geol. Soc. Am. Abstr. Programs 26, A-189.

Larson, N.W., 1979. Chronology of Late Cenozoic basaltic volcanism: The tectonic implications along a segment of the Sierra Nevada and Basin and Range Province boundary. Ph.D. thesis, Brigham Young University, Utah, 95 pp.

Locke, A., Billingsley, P.R., Mayo, E.B., 1940. Sierra Nevada tectonic patterns. Geol. Soc. Am. Bull. 51, 513–540.

Lombardi, O.W., 1957. Observations on the distribution of chemical elements in the terrestrial Saline Deposits of Saline Valley, California. M.S. thesis, New Mexico Institute of Mining and Technology, Socorro, New Mexico.

McAllister, J.F., 1956. Geology of the Ubehebe Peak Quadrangle, California. U.S. Geol. Surv. Quad. Map, GQ-95.

Menges, C.M., Oswald, J.A., Coe, J.A., Lundstrom, S.C., Paces, J.B., Mahan, S.A., Widmann, B., Murray, M., 1996. Paleoseismic investigations of Stagecoach Road fault, southeastern Yucca Mountain, Nye County, Nevada. U.S. Geol. Surv. Open-File Rep. 96-417, 71 pp.

O'Malley, P.A., 1980. Quaternary Geology and Tectonics of the Waucoba Wash 15-minute quadrangle, Saline Valley, Inyo County. M.S. thesis, University of Nevada Reno, Reno, 138 pp.

Oswald, J.A., 1998. Quaternary geology of southern Saline Valley and neotectonic character of the Hunter Mountain fault zone. M.S. thesis, University of Nevada Reno, Reno, 69 pp.

Pezzopane, S.K., Weldon, R.J., 1993. Tectonic role of active faulting in central Oregon. Tectonics 12, 1140–1169.

Reheis, M.C., 1991. Aerial photographic interpretation of lineaments and faults in Late Cenozoic deposits in the eastern parts of the Saline Valley 1:100,000 Quadrangle, Nevada and California, and the Darwin Hills 1:100,000 Quadrangle, California. U.S. Geol. Surv. Open-File Rep. 90-500.

Reheis, M.C., Dixon, T.H., 1996. Kinematics of the eastern California shear zone; evidence for slip transfer from Owens and Saline Valley fault zones to Fish Lake Valley fault zone. Geology 24, 339–342.

Sauber, J., 1990. Geodetic measurements of deformation in California. NASA Tech. Memo. 100732, 211.

Savage, J.C., Lisowski, M., 1990. Deformation in Owens Valley, California. Bull. Seismol. Soc. Am. 70, 1225–1232.

Savage, J.C., Lisowski, M., 1995. Strain accumulation in Owens Valley, California: 1974 to 1988. Bull. Seismol. Soc. Am. 85, 151–158.

Savage, J.C., Lisowski, M., Prescott, W.H., 1990. An apparent shear zone trending north–northwest across the Mojave Desert into Owens Valley. Geophys. Res. Lett. 17, 2113–2116.

Sawyer, T.L., 1991. Quaternary Geology and Tectonic Activity along the Fish Lake Valley Fault Zone, Nevada and California. M.S. thesis, University of Nevada Reno, Reno, 379 pp.

Smith, R.S.U., 1976. Late-Quaternary pluvial and tectonic history of Panamint Valley, Inyo and San Bernadino Counties, California. Ph.D. thesis, California Institute of Technology, Pasadena, 295 pp.

Stewart, J.H., 1980. Geology of Nevada. Nev. Bur. Mines Spec. Publ. no. 4, 136 pp.

Stewart, J.H., 1988. Tectonics of the Walker Lane belt, western Great Basin: Mesozoic and Cenozoic deformation in a zone of shear. In: Ernst, W.G. (Ed.), Metamorphism and Crustal Evolution of the Western United States. Prentice Hall, Englewood Cliffs, NJ, pp. 683–713.

Ward, S.N., 1990. Pacific-North America plate motions: new results from very long baseline interferometry. J. Geophys. Res. 95, 21965–21981.

Wells, S.G., McFadden, L.D., Dohrenwend, J.C., Bullard, T.F., Feilberg, B.F., Ford, R.L., Grimm, J.P., Miller, J.R., Orbock, S.M., Pickle, J.D., 1984. Late Quaternary geomorphic history of Silver Lake, eastern Mojave Desert, California: an example of the influence of climatic change on desert piedmonts. In: Dohrenwend, J.C. (Ed.), Surficial Geology of the Eastern Mojave Desert, California. Geol. Soc. Am. 1984 Annual Meetings Fieldtrip 14 Guidebook, Mackay School of Mines, Reno, NV, pp. 69–87.

Wells, S.G., McFadden, L.D., Dorn, R.L., DeNiro, M.J., Ajie, H.O., 1987. Isotopic evidence for climatic influence on alluvial-fan development in Death Valley, California, discussion and reply. Geology 15, 1178–1180.

Wesling, J.R., Bullard, T.F., Swan, F.H., Perman, R.C., Angel, M.M., Gibson, J.D., 1992. Preliminary mapping of surficial geology of Midway Valley, Yucca Mountain, Nye County, Nevada. Sandia National Laboratory Report SAND91-0607, Albuquerque, NM, 56 pp.

Wise, D.U., 1963. An outrageous hypothesis for the tectonic pattern of the North American Cordillera. Geol. Soc. Am. Bull. 74, 357–362.

Zellmer, J.T., 1980. Recent deformation in Saline Valley region, Inyo County, California. Ph.D. thesis, University of Nevada Reno, Reno.

Zhang, P., Ellis, M.A., Slemmons, D.B., Mao, F., 1990. Right-lateral displacements associated with prehistoric earthquakes and Holocene slip rate along the southern Panamint Valley fault zone: implications for southern Basin and Range tectonics. J. Geophys. Res. 95, 4857–4872.